LETTER

doi:10.1038/nature11894

Dynamics of a Snowball Earth ocean

Yosef Ashkenazy[1], Hezi Gildor[2], Martin Losch[3], Francis A. Macdonald[4], Daniel P. Schrag[4,5] & Eli Tziperman[4,5]

Geological evidence suggests that marine ice extended to the Equator at least twice during the Neoproterozoic era (about 750 to 635 million years ago)[1,2], inspiring the Snowball Earth hypothesis that the Earth was globally ice-covered[3,4]. In a possible Snowball Earth climate, ocean circulation and mixing processes would have set the melting and freezing rates that determine ice thickness[5,6], would have influenced the survival of photosynthetic life[4,5,7–9], and may provide important constraints for the interpretation of geochemical and sedimentological observations[4,10]. Here we show that in a Snowball Earth, the ocean would have been well mixed and characterized by a dynamic circulation[11], with vigorous equatorial meridional overturning circulation, zonal equatorial jets, a well developed eddy field, strong coastal upwelling and convective mixing. This is in contrast to the sluggish ocean often expected in a Snowball Earth scenario[3] owing to the insulation of the ocean from atmospheric forcing by the thick ice cover. As a result of vigorous convective mixing, the ocean temperature, salinity and density were either uniform in the vertical direction or weakly stratified in a few locations. Our results are based on a model that couples ice flow and ocean circulation, and is driven by a weak geothermal heat flux under a global ice cover about a kilometre thick. Compared with the modern ocean, the Snowball Earth ocean had far larger vertical mixing rates, and comparable horizontal mixing by ocean eddies. The strong circulation and coastal upwelling resulted in melting rates near continents as much as ten times larger than previously estimated[6,7]. Although we cannot resolve the debate over the existence of global ice cover[10,12,13], we discuss the implications for the nutrient supply of photosynthetic activity and for banded iron formations. Our insights and constraints on ocean dynamics may help resolve the Snowball Earth controversy when combined with future geochemical and geological observations.

The flow of thick ice over a Snowball Earth ocean ("sea glaciers", characterized by dynamics very different from that of thinner sea ice[14]), has received significant attention over the past few years[5–7,9,14,15]. Similarly, the role and dynamics of atmospheric circulation and heat transport, CO_2 concentration, cloud feedbacks, and continental configuration have been studied[16–18], as has the role of dust over the Snowball Earth's ice cover[17,19]. In contrast, despite its importance, the ocean circulation during Snowball Earth events has received little attention. The few studies that used full-ocean General Circulation Models concentrated mostly on the ocean's role in Snowball Earth initiation and aftermath[20,21]. No studies accounted for the combined effects of thick ice cover and flow, and driving by geothermal heating[11,13,22,23], yet ref. 11 simulated an ocean under a 200-m-thick ice cover with no geothermal heat flux, and described a non-steady-state solution with near-uniform temperature and salinity, and vanishing Eulerian circulation together with strong parameterized eddy-induced high-latitude circulation cells.

To allow us to simulate the special circumstances during Snowball Earth events, we use a novel model that couples the ocean and thick ice flow (see Methods). We begin by exploring the Snowball Earth circulation using an easier-to-understand two-dimensional (2D, latitude and depth) ocean model with no continents. The results point to the importance of ocean eddy motions, and given that these have never been studied for a Snowball Earth ocean, we investigate them using a high-resolution sector ocean model. Finally, we consider a near-global three-dimensional (3D) ocean model with reconstructed Neoproterozoic continental geometry to verify that our insights remain valid in this more realistic configuration.

We consider first the zonally averaged temperature, salinity and circulation, including the meridional overturning circulation (MOC). Figure 1 shows steady-state results from a 2D (latitude and depth) version of the ocean model coupled to a one-dimensional (1D, latitude) ice flow model, driven by geothermal heating (about 0.1 W m^{-2}) that is enhanced over a prescribed bottom ridge (Supplementary Fig. 2). We assume the presence of land ice at a volume equivalent to about one kilometre of sea level (Methods), and our model predicts that the upper kilometre of the ocean is frozen as well. Concentrating salt in a significantly lower ocean volume resulted in ocean salinity that is significantly higher than that of the present day (Fig. 1b). The high salinity and high pressure at the bottom of the ice lowered the freezing temperature to approximately -3.5° C, explaining the cold temperature field (Fig. 1a). Variations in temperature and salinity are fairly weak[11], as expected given the insulating thick ice cover and weak geothermal heat forcing.

The geothermal heat flux acts to create low-density water at the ocean bottom, and therefore leads to convective vertical mixing that makes the temperature and salinity effectively vertically uniform nearly everywhere, creating a water-mass pattern that is completely different from that expected during any other period in Earth history (Fig. 1a, b). Near the enhanced geothermal heating over the ridge, there is a weakly stable stratification due to meltwater production over the enhanced heating (bounded by the thick black contour in Fig. 1a, b).

The MOC (Fig. 1d) is surprisingly strong and is confined to around the Equator, very different from the high-latitude present-day MOC. The meridional velocity, which together with the vertical velocity composes the MOC, therefore decays very rapidly away from the Equator. The most prominent features in the zonal velocity field are the two strong jet-like flows near the Equator, flowing at opposite directions on the two sides of the Equator, and decaying slowly away from the Equator (Fig. 1c). The zonal velocity in the higher latitudes, away from the equatorial jet-like structures, is generally eastward throughout most of the water column apart from near the bottom. This eastward mid- to high-latitude velocity is in geostrophic equilibrium between the Coriolis force and the pressure gradient, and is driven by the large-scale meridional pressure and hence by the density gradient (which is a consequence of heating and melting over the ridge, lowering the density there; Methods).

To understand the equatorial zonal flows and MOC, we note that their dominant momentum balance is geostrophic in the north–south direction, and hydrostatic in the vertical, as is the case in the present-day ocean. The east–west momentum balance, however, is between the Coriolis force and eddy (turbulent) viscosity, which is negligible in most of the present-day ocean. The dominant momentum balances are therefore:

[1]Department of Solar Energy and Environmental Physics, The Blaustein Institutes for Desert Research, Ben-Gurion University of the Negev, Midreshet Ben-Gurion, 84990, Israel. [2]Institute of Earth Sciences, The Hebrew University of Jerusalem, Jerusalem, 91904, Israel. [3]Alfred-Wegener-Institut für Polar- und Meeresforschung, 27515 Bremerhaven, Germany. [4]Earth and Planetary Sciences, Harvard University, 20 Oxford Street, Cambridge, Massachusetts 02138, USA. [5]School of Engineering and Applied Sciences, Harvard University, 20 Oxford Street, Cambridge, Massachusetts 02138, USA.

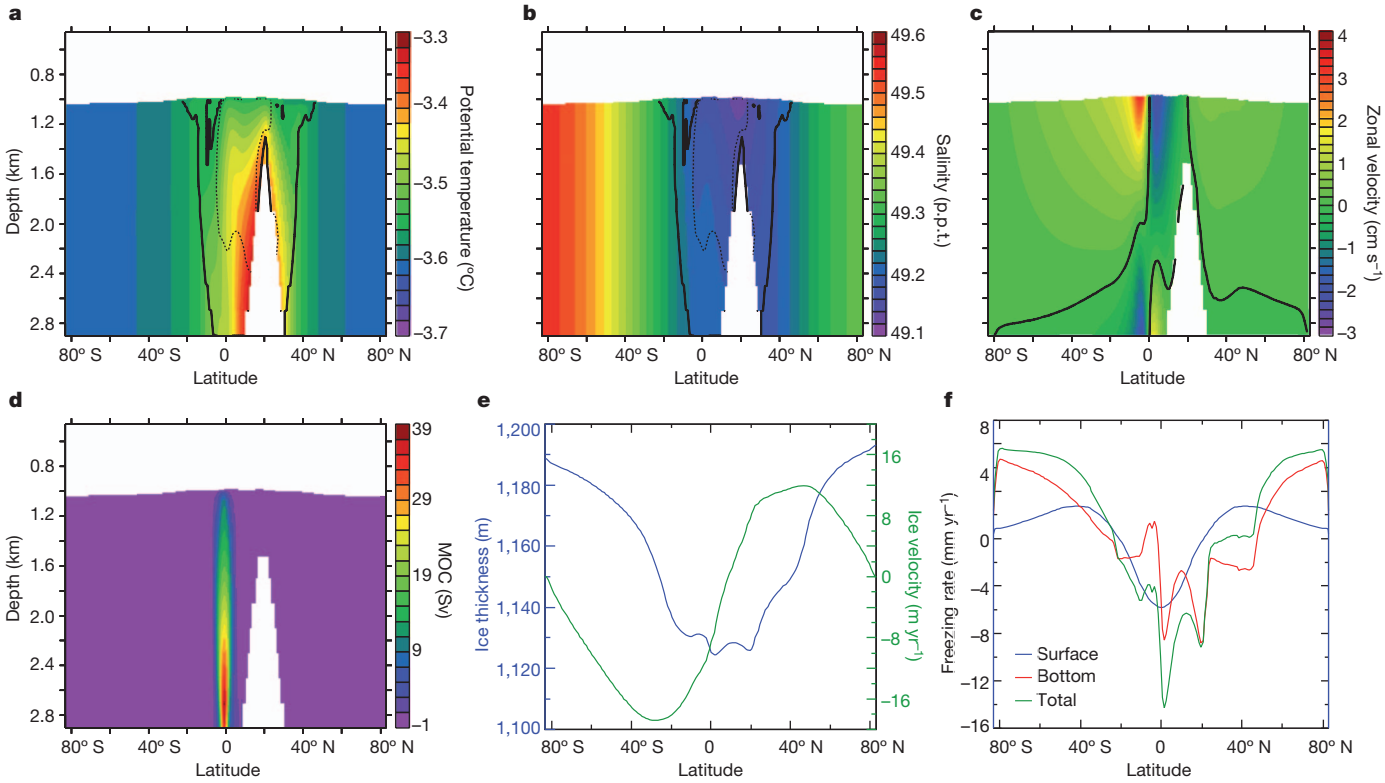

Figure 1 | Results of a 2D (latitude and depth) ocean model coupled to a 1D (latitude only) ice flow model. **a**, Potential temperature (colour scale; white area on top corresponds to the calculated ice cover thickness). **b**, Salinity (colour scale, in parts per thousands, p.p.t.), which varies due to freezing and melting (**f**) induced by spatially variable geothermal heating and heat flux through the ice owing to the latitude-dependent atmospheric temperature (Methods); salinity is somewhat lower in the Northern Hemisphere because of the ridge with enhanced geothermal heating and therefore enhanced melting there. **c**, Zonal velocity (colour scale). **d**, MOC stream function (colour scale; 1 Sv = 10^6 m^3 s^{-1}), showing a strong equatorial MOC (35 Sv), compared to the present-day high-latitude North Atlantic MOC (about 20 Sv). **e**, Ice thickness and ice velocity as functions of latitude. **f**, Freezing rate (negative values imply melting) at the ice base together with prescribed sublimation/precipitation rates at the ice surface, showing that ocean contribution to setting the ice thickness is comparable to or larger than that of the atmosphere.

$$-fv = \nu_h u_{yy}$$
$$fu = -p_y/\rho_0$$
$$p_z = -g\rho$$

where the east, north and vertical coordinates and velocities are denoted (x, y, z) and (u, v, w), g is gravitational acceleration, $\nu_h = 2 \times 10^4$ m^2 s^{-1} the horizontal eddy viscosity coefficient, $f \approx \beta y$ is the Coriolis parameter, using the equatorial β plane approximation, ρ is the density, ρ_0 a reference density, and p is the pressure. The meridional scale obtained from the zonal momentum equation is $L \approx (\nu_h/\beta)^{1/3} \approx 100$ km, consistent with the extent of the MOC in the numerical solution. Assuming the meridional pressure gradient set by the differential geothermal heating to be approximately constant in latitude near the Equator, we can solve the above equations (Methods) to find:

$$u \approx [g\rho_y(z + H/2)/(\beta\rho_0)](1/y)$$
$$v \approx -[2\nu_h g\rho_y(z + H/2)/(\beta^2\rho_0)](1/y^4)$$

where H is the ocean depth. The more rapid decay of the meridional velocity v as function of latitude y in these expressions explains why the MOC is restricted to the equatorial region, while the equatorial zonal flows u extend farther poleward. These solutions also predict that u changes sign across the Equator (where $y = 0$) but v does not, and also that both horizontal velocities change sign with depth, at $z = -H/2$, all remarkably consistent with Fig. 1c, d.

The ice thickness in these solutions (Fig. 1e) is quite uniform, varying from 1,120 m to 1,200 m, owing to the homogenizing effect of the ice flow[6], consistent with previous studies[7,15]. High-latitude basal freezing and low-latitude melting rates are balanced by an equatorward ice flow and are comparable to, if not larger than, the ice surface sublimation and precipitation rates (Fig. 1f). These rates are quite different from previous estimates that ignored ocean dynamics[7], highlighting the important role of ocean dynamics.

The above 2D model predicts the ocean turbulent eddy field to have a dominant role in the momentum budget, via its parameterization by the horizontal eddy viscosity ν_h. Snowball Earth eddy motions have not been studied before to our knowledge, and to examine them, we considered the results of a high-resolution model, shown in Fig. 2. This model demonstrated that the solution for the ocean circulation is surprisingly turbulent and time-dependent, far from the stagnant Snowball Earth ocean one might envision given the lack of wind forcing and air–sea fluxes. The zonal velocity field (Fig. 2c, f) shows several strong jets off the Equator, in addition to the two equatorial jets seen in the 2D solution. These jets, reminiscent of those seen in the atmosphere of Jupiter, arise from the action of the eddies. That is, the equatorial flows are unstable and generate eddies; the meridional convergence of eddy momentum fluxes $\partial\overline{u'v'}/\partial y$ generates additional jets off the Equator (Fig. 2f), which again are unstable and feed back on the eddies that sustain the jets[24].

The high-resolution run also shows a warm area to the northwest of the land mass, which leads to local melting rates of up to 10 cm yr^{-1} (Fig. 2e), about ten times larger than the maximum melting rates calculated by coarse model runs[6,7]. This warmer area is due to a concentrated coastal upwelling of deep water heated by geothermal heating. The upwelling occurs in response to the equatorial zonal flow away from the continent. This deep heating is allowed by a very weak

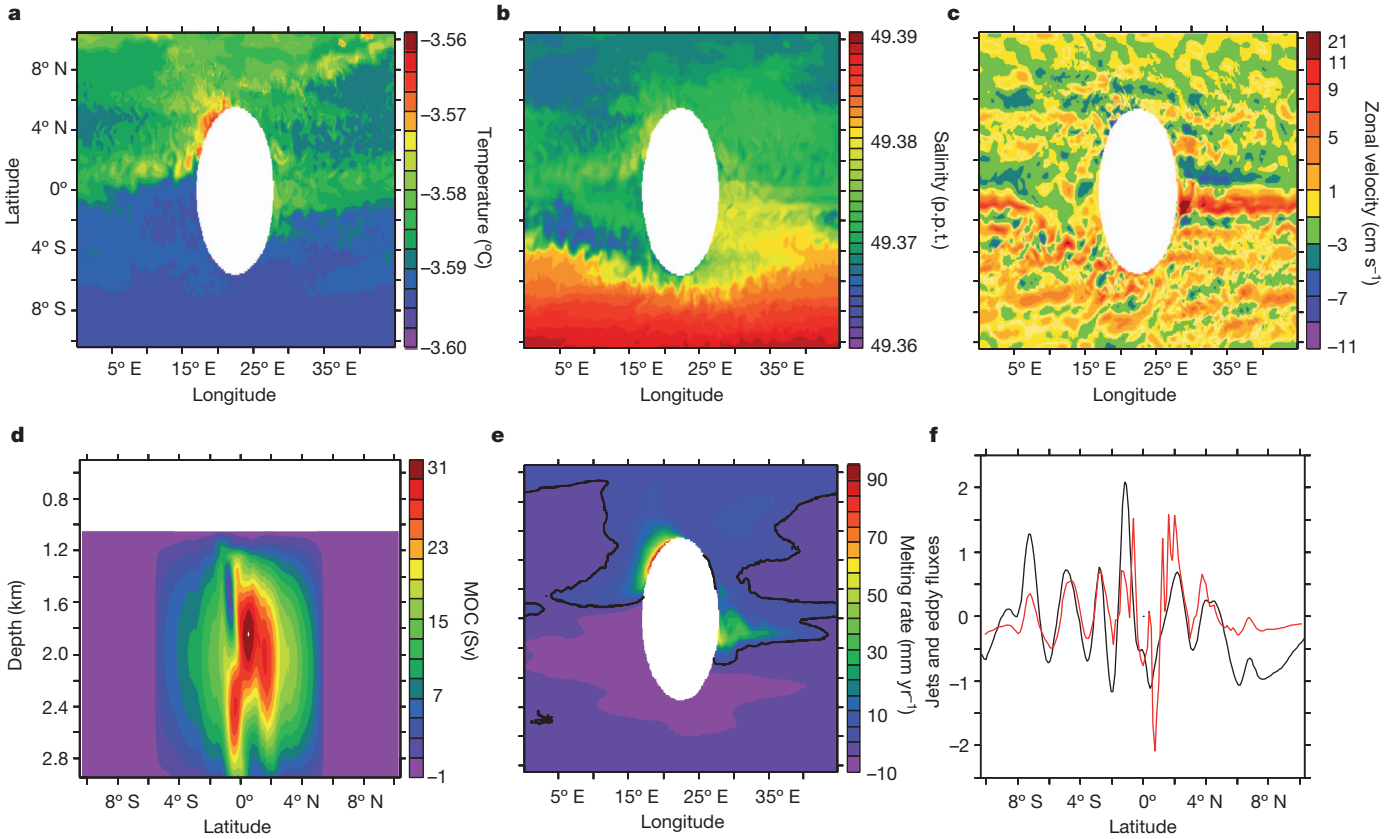

Figure 2 | Results of a 3D high-resolution sector ocean model showing a rich time-dependent turbulent eddy field. **a**, Snapshot of the temperature field (colour scale) at 1,150 m (that is, 125 m below the ice). **b**, As for **a**, but for salinity (colour scale). **c**, As for **a**, but for zonal velocity (colour scale). **d**, Time-averaged MOC (colour scale). **e**, Time-averaged melting rate (colour scale; zero values marked by thick black contour). **f**, Zonal, depth and time means of zonal velocity (black), and of scaled convergence of eddy momentum fluxes $-\partial\overline{u'v'}/\partial y$ (red), both as function of latitude. The close correspondence between the two demonstrates that eddy momentum flux convergence has a dominant role in the generation of the zonal jets.

local salinity-induced stratification due to geothermally driven ice melting (similar to that seen over the ridge in Fig. 1b). Although it is intriguing, the prescribed ice thickness in this model does not allow us to use this large melting rate conclusively to deduce the existence of thin ice or open water locally near continents, as suggested by some observations[10], and to explain the survival of photosynthetic life during a global Snowball Earth[8,9,15,25]. The explicitly resolved eddy field can be used to estimate a mixing timescale from low to high latitudes of 500 years (Methods), which is not very different from present-day basin-scale mixing rates.

Finally, a 3D ocean solution with a realistic continental configuration supports the results of the 2D model (Fig. 3a, b and Supplementary Fig. 3). The zonally averaged fields (Supplementary Fig. 3), equatorial zonal jets, large-scale westward flows in the higher latitudes, the existence of an equatorial MOC, and the vertically uniform temperature, salinity and density in most areas away from the enhanced geothermal heating, are all consistent with the 2D solution discussed above. Differences from the 2D case include a weaker salinity range due to the concentrated geothermal heating region being confined and therefore weaker in the 3D case (spatial average is 0.1 W m^{-2} in both); the equatorial MOC is composed of two cells owing to the more complex continental and geothermal heating configuration. Like the high-resolution model discussed above, the global 3D solution in the presence of continents shows upwelling and downwelling wherever the equatorial zonal jets encounter continents. This upwelling is possibly due to the weak stratification of the Snowball Earth ocean, whereas in an ocean with present-day like stratification these jets would be diverted sideways via horizontal boundary currents.

The weakly stratified, convectively mixed ocean found here, as well as the strong coastal upwelling, strong equatorial MOC and well developed eddy field, all imply that the deep and surface ocean are strongly linked in a Snowball Earth scenario, unlike in the well stratified present-day ocean. The well-mixed Snowball Earth ocean[11] has several interesting geochemical implications. First, if there are areas of photosynthesis under a local patch of thin ice, mixing or upwelling are needed to resupply limiting nutrients, because a weakly mixed ocean would lead to the exhaustion of the local nutrient pool and productivity would end. Second, the return of banded iron formations after a billion-year absence is an iconic feature of Neoproterozoic glaciation that is often attributed to stagnant Snowball Earth deep water[3]. Assuming that melt water was derived from land ice that contained air bubbles of an oxygenated atmosphere, one might expect that with enhanced melting and a strongly mixed ocean, iron concentrations could not rise sufficiently to deposit banded iron formations. However, Neoproterozoic banded iron formations, unlike Archean and Palaeoproterozoic ones, are not broadly distributed[26]. Instead, they form irregular lenticular bodies within glacial deposits, and are found predominantly in juvenile rift basins in close association with volcanic rocks, analogous to the Red Sea, where iron is supplied by hydrothermal fluids[27]. Such rift basins are somewhat isolated from the rest of the well-mixed ocean, allowing the build-up of iron levels and the development of banded iron formations, not inconsistent with our results showing a well-mixed ocean.

Our findings suggest that beneath the Snowball Earth ice cover, the Neoproterozoic oceans were dynamic, well mixed[11] and spatially and temporally variable: far from a stagnant pool. These ocean dynamics insights open the way to a reinterpretation of some geochemical, sedimentary and paleontological observations, possibly contributing to the debate on the existence of a global ice cover and to our understanding of the Neoproterozoic era.

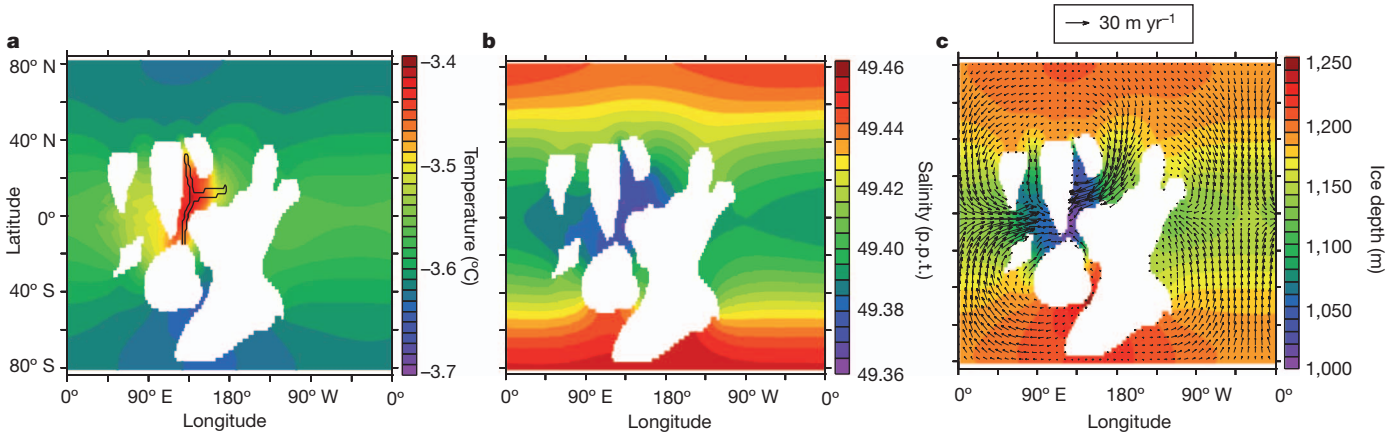

Figure 3 | Results of the 3D ocean model coupled to a 2D (latitude and longitude) ice flow model, in the presence of reconstructed Neoproterozoic continental configuration. **a**, Temperature at 1,200 m depth (colour scale), areas of enhanced geothermal heating (black contour lines) and land masses (white areas). **b**, Salinity at 1,200 m (colour scale). **c**, Ice thickness (colour scale), and ice velocity vectors (plotted every fourth grid point in the longitude direction and every second grid point in the latitude direction). Results are generally consistent with the 2D solution (see also Supplementary Fig. 3), although some deviations from zonal symmetry occur owing to advection of temperature and salinity by ocean currents near continents, and owing to enhanced heating and freshening via ice melting in the area of enhanced geothermal heating between the continents.

METHODS SUMMARY

Our model couples the state-of-the-art ocean general circulation model, MITgcm[28], which can simulate thick ice shelves[29], with a recently developed 2D (latitude and longitude) ice flow model[15], extending previous 1D flow models[6,7]. The model is run here in three configurations: 2D (latitude and depth) ocean model coupled to a 1D (latitude) ice flow model; a high-resolution (1/8°) sector model with prescribed uniform ice cover; and a 3D global model with reconstructed Neoproterozoic continental configuration coupled to a 2D ice flow model. A geothermal heat flux is prescribed in all three versions at the bottom of the ocean (Supplementary Fig. 2), with a spatial average of 0.1 W m^{-2}, and is spatially uniform except not far from the Equator (motivated by the Neoproterozoic continental reconstruction of ref. 30), where the geothermal flux is up to four times its background value. The 2D ocean model also prescribes a ridge over which the heating is enhanced, while the topography of the two other models is flat. Sensitivity experiments to the location and amplitude of the enhanced heating, and to the topography in both the 2D and 3D models, show our solution to be very robust.

Full Methods and any associated references are available in the online version of the paper.

Received 18 September 2012; accepted 8 January 2013.

1. Harland, W. B. in *Problems in Palaeoclimatology* (ed. Nairn, A. E. M.) 119–149 180–184 (John Wiley & Sons, 1964).
2. Evans, D. A. D. & Raub, T. D. in *The Geological Record of Neoproterozoic Glaciations* (eds Arnaud, E., Halverson, G. P. & Shields-Zhou, G.) Vol. 36, 93–112 (London, Geological Society of London, 2011).
3. Kirschvink, J. in *The Proterozoic Biosphere: A Multidisciplinary Study* (eds Schopf, J. & Klein, C.) 51–52 (Cambridge University Press, 1992).
4. Hoffman, P. & Schrag, D. The snowball Earth hypothesis: testing the limits of global change. *Terra Nova* **14,** 129–155 (2002).
5. McKay, C. Thickness of tropical ice and photosynthesis on a snowball Earth. *Geophys. Res. Lett.* **27,** 2153–2156 (2000).
6. Goodman, J. & Pierrehumbert, R. Glacial flow of floating marine ice in "Snowball Earth". *J. Geophys. Res.* **108,** doi:10.1029/2002JC001471 (2003).
7. Pollard, D. & Kasting, J. Snowball Earth: a thin-ice solution with flowing sea glaciers. *J. Geophys. Res.* **110,** doi:10.1029/2004JC002525 (2005).
8. Corsetti, F., Olcott, A. & Bakermans, C. The biotic response to Neoproterozoic snowball Earth. *Palaeogeogr. Palaeoclimatol. Palaeoecol.* **232,** 114–130 (2006).
9. Campbell, A. J., Waddington, E. D. & Warren, S. G. Refugium for surface life on Snowball Earth in a nearly-enclosed sea? A first simple model for sea-glacier invasion. *Geophys. Res. Lett.* **38,** doi:10.1029/2011GL048846 (2011).
10. Allen, P. A. & Etienne, J. L. Sedimentary challenge to Snowball Earth. *Nature Geosci.* **1,** 817–825 (2008).
11. Ferreira, D., Marshall, J. & Rose, B. Climate determinism revisited: multiple equilibria in a complex climate model. *J. Clim.* **24,** 992–1012 (2011).
12. Pierrehumbert, R. T., Abbot, D. S., Voigt, A. & Koll, D. Climate of the Neoproterozoic. *Annu. Rev. Earth Planet. Sci.* **39,** 417–460 (2011).
13. Yang, J., Peltier, W. R. & Hu, Y. The initiation of modern "Soft Snowball" and "Hard Snowball" climates in CCSM3. Part II: Climate dynamic feedbacks. *J. Clim.* **25,** 2737–2754 (2012).
14. Warren, S., Brandt, R., Grenfell, T. & McKay, C. Snowball Earth: ice thickness on the tropical ocean. *J. Geophys. Res.* **107,** doi:10.1029/2001JC001123 (2002).
15. Tziperman, E. *et al.* Continental constriction and sea ice thickness in a Snowball-Earth scenario. *J. Geophys. Res.* **117,** doi:10.1029/2011JC007730 (2012).
16. Pierrehumbert, R. Climate dynamics of a hard snowball Earth. *J. Geophys. Res.* **110,** doi:10.1029/2004JD005162 (2005).
17. Le Hir, G., Donnadieu, Y., Krinner, G. & Ramstein, G. Toward the snowball earth deglaciation. *Clim. Dyn.* **35,** 285–297 (2010).
18. Donnadieu, Y., Goddéris, Y., Ramstein, G., Nédélec, A. & Meert, J. A snowball Earth climate triggered by continental break-up through changes in runoff. *Nature* **428,** 303–306 (2004).
19. Abbot, D. S. & Pierrehumbert, R. T. Mudball: surface dust and Snowball Earth deglaciation. *J. Geophys. Res.* **115,** doi:10.1029/2009JD012007 (2010).
20. Poulsen, C., Pierrehumbert, R. T. & Jacobs, R. L. Impact of ocean dynamics on the simulation of the Neoproterozoic "snowball Earth". *Geophys. Res. Lett.* **28,** 1575–1578 (2001).
21. Poulsen, C. & Jacob, R. Factors that inhibit snowball Earth simulation. *Paleoceanography* **19,** doi:10.1029/2004PA001056 (2004).
22. Voigt, A., Abbot, D. S., Pierrehumbert, R. T. & Marotzke, J. Initiation of a Marinoan Snowball Earth in a state-of-the-art atmosphere-ocean general circulation model. *Clim. Past* **7,** 249–263 (2011).
23. Le Hir, G., Ramstein, G., Donnadieu, Y. & Pierrehumbert, R. T. Investigating plausible mechanisms to trigger a deglaciation from a hard snowball Earth. *C. R. Geosci.* **339,** 274–287 (2007).
24. Farrell, B. F. & Ioannou, P. J. Structural stability of turbulent jets. *J. Atmos. Sci.* **60,** 2101–2118 (2003).
25. Runnegar, B. Palaeoclimate: loophole for snowball Earth. *Nature* **405,** 403–404 (2000).
26. Bekker, A. *et al.* Iron formation: the sedimentary product of a complex interplay among mantle, tectonic, oceanic, and biospheric processes. *Econ. Geol.* **105,** 467–508 (2010).
27. Young, G. M. Proterozoic plate tectonics, glaciation and iron-formations. *Sedim. Geol.* **58,** 127–144 (1988).
28. Marshall, J., Adcroft, A., Hill, C., Perelman, L. & Heisey, C. A finite-volume, incompressible Navier Stokes model for studies of the ocean on parallel computers. *J. Geophys. Res.* **102,** 5753–5766 (1997).
29. Losch, M. Modeling ice shelf cavities in a z coordinate ocean general circulation model. *J. Geophys. Res.* **113,** doi:10.1029/2007JC004368 (2008).
30. Li, Z. X. *et al.* Assembly, configuration, and break-up history of Rodinia: a synthesis. *Precambr. Res.* **160,** 179–210 (2008).

Supplementary Information is available in the online version of the paper.

Acknowledgements We thank B. Rose for comments. This work was supported by the NSF Climate Dynamics P2C2 programme, grant number ATM-0902844 (to E.T. and Y.A.). E.T. thanks the Weizmann Institute for its hospitality during parts of this work. Y.A. thanks the Harvard EPS department for a most pleasant and productive sabbatical visit.

Author Contributions Y.A. and E.T. formulated the problem and performed the model runs and analysis, F.A.M. and D.P.S. contributed to the geological motivation and interpretation, M.L. and H.G. helped with the model set-up, and all authors contributed to the writing of the manuscript.

Author Information Reprints and permissions information is available at www.nature.com/reprints. The authors declare no competing financial interests. Readers are welcome to comment on the online version of the paper. Correspondence and requests for materials should be addressed to E.T. (eli@eps.harvard.edu) or Y.A. (ashkena@bgu.ac.il).

METHODS

Model description. The model used here couples the Massachusetts Institute of Technology general circulation ocean model (MITgcm)[28] with its ice-shelf package[29] to a recently developed 2D (latitude and longitude) model of thick ice flow over a Snowball Earth ocean[15], which is an extension of the 1D ice flow model of refs 6 and 7 and similar ones[31–33]. The ice flow model compensates for melting and sublimation at low latitudes and freezing/precipitation at high latitudes, with an equatorward ice flow calculated from ice-thickness gradients based on Glenn's law. The ice flow model employs the well known ice-shelf approximation in which the velocity is independent of depth[34,35], together with an assumed linear vertical temperature profile within the ice[6], which together make it possible to average over the vertical dimension rather than model it explicitly.

The coupling of the ice and ocean models is done asynchronously: the ocean model is run for 300 years and the ice model is then run for a similar period, and the process is repeated until a steady state is obtained. At each iteration the ocean model is given the ice thickness calculated by the ice model, while the ice model is driven by the melting and freezing rates calculated by the ocean model. The ice-surface meridional temperature, sublimation and snowfall are taken from ref. 7, with an Equator-to-pole temperature difference of 36° C (Supplementary Fig. 1). No-slip ocean boundary conditions are specified on side and bottom boundaries, and free-slip conditions are specified under the ice cover.

Turbulent convection is parameterized in our model experiments by an increased vertical diffusion where the vertical stratification is unstable. Eddy mixing and mixed-layer parameterizations developed for the present-day ocean[36] are probably not applicable for the very weakly stratified Snowball Earth ocean, and we use instead crude horizontal and vertical eddy diffusion. A different choice was made by ref. 11, who used an eddy parameterization tuned to present-day ocean eddies[36] and simulated a Snowball Earth ocean under 200-m-thick ice with no geothermal heating and therefore not at a thermodynamic equilibrium, but with a quasi-equilibrated circulation. They found a very weakly stratified ocean and described a vanishing Eulerian velocity field, yet with strong high-latitude parameterized eddy-driven meridional circulation cells, very different from the vigorous Eulerian equatorial overturning and jets we found here.

The 2D ocean model uses a horizontal diffusion coefficient of $\kappa_h = 200\,m^2\,s^{-1}$ and viscosity of $\nu_h = 2\times10^4\,m^2\,s^{-1}$; the 3D "realistic geometry" case uses different values of $\kappa_h = 500\,m^2\,s^{-1}$ and $\nu_h = 5\times10^4\,m^2\,s^{-1}$ required by its different resolution. The vertical viscosity in both models is set to $\nu_v = 2\times10^{-3}\,m^2\,s^{-1}$ and the vertical diffusivity to $\kappa_v = 1\times10^{-4}\,m^2\,s^{-1}$. The high-resolution case uses a Leith eddy viscosity formulation[37].

The 2D ocean model (latitude and depth, periodic in longitude) has a horizontal latitudinal resolution of 1° and 32 vertical levels, varying in thickness from 10 m adjacent to the ice to 200 m at depth (vertical grid spacing varies from 920 m at the top, entirely within the ice, followed by 15 levels of 10 m thickness each, and then 12 m, 17 m, 23 m, 32 m, 45 m, 61 m, 82 m, 110 m, 148 m, and seven levels of thickness 200 m at the bottom). The 2D ocean model is coupled to a 1D (latitude) version of the ice flow model. We performed sensitivity runs to the location and amplitude of the geothermal forcing and found the solution to be very robust.

The 3D near-global ocean model was run at a horizontal resolution of 2° from 82° S to 82° N, and with 73 vertical levels of varying thickness from 10 m near the ice to 200 m at depth (starting from the ocean surface, the first level is 550 m thick, followed by 57 levels whose thickness is 10 m, and then 14 m, 20 m, 27 m, 38 m, 54 m, 75 m, 105 m, 147 m, and finally seven levels of thickness 200 m; at steady state, the upper 33 levels are within the ice, and therefore inactivated, and the rest represent the ocean). Continental configuration is based on the 720-million-year-old Neoproterozoic reconstruction of ref. 30, and includes an estimated location of spreading ridges between the continents, where geothermal heating is probably enhanced (thick black contour in Fig. 3a; spreading ridges elsewhere are not included owing to the uncertainty in their location). Bathymetry reconstructions for the Neoproterozoic are not easy to come by, and we therefore specified a flat topography in the 3D case, relying on land masses to restrict zonal flows. We performed sensitivity runs with specified sills (1 km high) around the ocean constricted by the land masses, as well as with (1 km high) mid-ocean ridges specified in the open ocean, and found that these do not change the overall picture.

The high-resolution sector ocean model spans 45° longitude, from 10.5° S to 10.5° N, at a horizontal resolution of an eighth of a degree longitude and latitude and 20 vertical levels of thickness 100 m each. An ice cover with uniform thickness of 1,025 m is prescribed in this case rather than using the ice flow model (which would be prohibitive owing to the computational cost). A flat ocean topography is used, and enhanced geothermal heating is prescribed as a Gaussian centred around 6° N, at up to four times the amplitude of the background geothermal flux. The surface temperature in this experiment is uniform (due to its relatively small meridional extent) and set to −44.4° C. This high-resolution run was integrated for over 100 years to reach an equilibrium of the eddy field, yet because its ice cover is specified rather than evolving, the run is—unlike for the other two models—not at a complete thermodynamic equilibrium with its ice cover.

While geothermal heat can have some effect on the present-day ocean[38], it is the dominant forcing in a Snowball Earth ocean. A hydrothermal heat flux is therefore prescribed here at the bottom of the ocean and is spatially uniform except where enhanced flux is prescribed to simulate the effect of spreading ridges. These enhanced geothermal areas are prescribed in the model runs shown in the paper to be not far from the Equator (motivated by the Neoproterozoic continental reconstruction of ref. 30), and the geothermal flux there is up to four times its background value. The observed background flux away from ocean ridges is about $0.05\,W\,m^{-2}$, and the flux observed at mid-ocean ridges is about four times larger, such that the average over ocean basins is estimated to be of the order of $0.1\,W\,m^{-2}$ (see, for example, table 4 of ref. 39). We therefore prescribe a flux whose spatial average is $0.1\,W\,m^{-2}$, and which is larger locally over ridges. At a steady state the average flux escaping the ocean through the thick ice cover is therefore also $0.1\,W\,m^{-2}$. Supplementary Fig. 2 shows the hydrothermal forcing of all three models shown in the paper. The Neoproterozoic flux may have been slightly larger than that of the present day, but the difference is expected to be small relative to other uncertainties, so that modern values are used here.

Most ocean models cannot incorporate an ice cover thicker than their upper level, which is of the order of 5–50 m. It is, however, important to use a thick shelf ice formulation as done here, given that representing thick ice-shelves as thin sea ice is known to lead to biases in modelling present-day deep-water formation around Antarctica owing to the induced biases in freshwater fluxes due to melting/freezing[40,41]. An alternative to our thick ice-shelf formulation was used by ref. 11, which employed a dynamic rescaling of the vertical coordinate[42].

Derivation of the solution for the 2D flow field. Consider the zonal equatorial jets seen (for example) in Fig. 1. Differentiate the hydrostatic equation in y and integrate in z to find $p_y = g\rho_y z + F(y)$, and assume this meridional pressure gradient set by the differential geothermal heating to be approximately constant in latitude y around the Equator. The meridional momentum equation then leads to an expression for u, and the zonal momentum equation to an expression for v. Requiring the vertically integrated meridional flow to vanish owing to mass conservation, we find $F(y)$, giving:

$$u \approx [g\rho_y(z + H/2)/(\beta\rho_0)](1/y)$$

$$v \approx -[2\nu_h g\rho_y(z + H/2)/(\beta^2\rho_0)](1/y^4)$$

If the geothermal heating and bathymetry are prescribed to be uniform, the MOC is weaker by about 75%, and if the ice-surface meridional temperature is also uniform, the MOC vanishes. This suggests that the atmospheric forcing via the ice-surface meridional temperature is responsible for about 25% of the MOC, in spite of the thick ice cover. The atmospheric driving of the Snowball Earth ocean, and of the MOC in particular, is through its effect on melting rates at high versus low latitudes. This difference mostly depends on the Equator-to-pole atmospheric temperature difference, and if the carbon dioxide is increased, for example, and if the meridional temperature difference is consequently lowered, then the atmospheric driving of the ocean circulation may be weaker. In addition to this, the sensitivity of the ice flow to surface temperatures derived from different carbon dioxide concentrations was explicitly discussed by ref. 15. When the geothermal forcing is uniform (but the ice-surface meridional temperature is still a function of latitude y), or the ridge with enhanced heating is placed at the Equator, the north–south symmetry is still broken, and although the MOC is weaker and could be in either direction depending on initial conditions, the flows are qualitatively similar to the above.

On the eddy field in the high-resolution model run. The relatively strong zonal velocities that develop in the above 2D model near the Equator are characterized by a Reynolds number (based on molecular viscosity) that is much greater than one, of $R = uL/\nu = (0.03\,m\,s^{-1})(2\times10^5\,m)/(1.8\times10^{-6}\,m^2\,s^{-1}) \approx 4\times10^9$, anticipating a turbulent flow. In addition, the meridional gradient of vorticity ($\beta - u_{yy}$) changes sign as function of latitude, indicating that eddies may develop owing to barotropic instability. It is also possible that the eddy field may be able to extract available potential energy from the (weak) meridional density gradient.

The eddy motions seen in our high-resolution run are characterized by a velocity scale of $u' \approx 0.02\,m\,s^{-1}$ and a length scale of $l \approx 100$ km (Fig. 2c). These scales can be used to estimate a mixing-length eddy viscosity of $\nu_h \approx u'l \approx 2\times10^3\,m^2\,s^{-1}$. A mixing timescale from low to high latitudes is therefore given by $\tau \approx R^2/\nu_h \approx$ 500 years, where R is the Earth's radius, not very different from present-day basin-scale mixing rates. This is a lower bound on mixing timescales, because one expects the snowball eddy field to be weaker at the higher latitudes where the mean flows and resulting eddy field are weaker. This is in contrast to the present-day ocean,

where eddy generation is strong at mid- to high latitudes near western boundary currents.

Salinity uncertainties. Estimating ocean salinity during the Neoproterozoic presents a challenge. We assume the pre-Snowball Earth salinity to be equal to that of the present day, but there is significant evidence that it varied significantly and may have been as high as twice that of the present day[43]; see also some recent reviews of evaporites through time[44,45]. Salinity may also have increased during Snowball Earth events if oceans continued to receive a supply of salts through both subglacial runoff and subglacial sediment transport, whereas evaporite deposition would have been nonexistent. The main effect of a higher ocean salinity on our simulation would have been the additional lowering of the freezing temperature, which is already quite low relative to modern values owing to both high pressure at the ice base and high salinity.

Another source of uncertainty in salinity is our assumed concentration of salt as a result of land-ice volume being equivalent to about 1 km of sea level. Modelling studies[46,47] estimate continental ice sheets to be a few kilometres thick after about 100,000 years, roughly comparable to the East Antarctic Ice-Sheet with a mean thickness of 2.15 km (ref. 48). In addition, geological relationships[49] estimated a post-glacial sea-level rise of 1.5 km, which is equivalent to melting 3.3-km-thick grounded ice sheets on all continents and oceanic platforms. We conclude that although no tight constraint on land ice exists, 1-km-thick ice sheets seem to be within the range of current estimates.

Yet another important salinity-related issue is the possibility of freshwater input from land-based subglacial flows. Such freshwater flow at the ocean surface, which may develop should there be any open coastal water, could be mixed down by the strong vertical convective mixing. Yet, if the fresh water input is strong enough, it could lead to a weak local coastal stratification (as seen in our solution) over the ridge due to melting there (Fig. 1b). This scenario remains speculative, given that it hinges on the existence of open coastal water, which our model does not explicitly predict.

31. Li, D. & Pierrehumbert, R. T. Sea glacier flow and dust transport on Snowball Earth. *Geophys. Res. Lett.* **38,** doi:10.1029/2011GL048991 (2011).
32. Goodman, J. C. Through thick and thin: marine and meteoric ice in a "Snowball Earth" climate. *Geophys. Res. Lett.* **33,** doi:10.1029/2006GL026840 (2006).
33. Pollard, D. & Kasting, J. F. Reply to comment by Stephen G. Warren and Richard E. Brandt on "Snowball Earth: A thin-ice solution with flowing sea glaciers". *J. Geophys. Res.* **111,** doi:10.1029/2006JC003488 (2006).
34. Morland, L. Unconfined ice-shelf flow. In *Dynamics of the West Antarctic Ice Sheet* (eds van der Veen, C. & Oerlemans, J.) 99–116 (D. Reidel, 1987).
35. MacAyeal, D. EISMINT: Lessons in ice-sheet modeling. Technical Report http://geosci.uchicago.edu/pdfs/macayeal/lessons.pdf (University of Chicago, 1997).
36. Gent, P. R. & McWilliams, J. C. Isopycnal mixing in ocean circulation models. *J. Phys. Oceanogr.* **20,** 150–155 (1990).
37. Leith, C. E. Stochastic models of chaotic systems. *Physica D* **98,** 481–491 (1996).
38. Adcroft, A., Scott, J. R. & Marotzke, J. Impact of geothermal heating on the global ocean circulation. *Geophys. Res. Lett.* **28,** 1735–1738 (2001).
39. Pollack, H., Hurter, S. & Johnson, J. Heat flow from the Earth's interior: analysis of the global data set. *Rev. Geophys.* **31,** 267–280 (1993).
40. Hellmer, H., Schodlok, M., Wenzel, M. & Schröter, J. On the influence of adequate Weddell Sea characteristics in a large-scale global ocean circulation model. *Ocean Dyn.* **55,** 88–99 (2005).
41. Thoma, M., Grosfeld, K. & Lange, M. The impact of the Eastern Weddell ice shelves on water masses in the Eastern Weddell Sea. *J. Geophys. Res.* **111,** C12010 (2006).
42. Campin, J., Marshall, J. & Ferreira, D. Sea ice–ocean coupling using a rescaled vertical coordinate z. *Ocean Model.* **24,** 1–14 (2008).
43. Knauth, L. Temperature and salinity history of the Precambrian ocean: implications for the course of microbial evolution. *Palaeogeogr. Palaeoclimatol. Palaeoecol.* **219,** 53–69 (2005).
44. Warren, J. Evaporites through time: tectonic, climatic and eustatic controls in marine and nonmarine deposits. *Earth Sci. Rev.* **98,** 217–268 (2010).
45. Evans, D. A. D. Proterozoic low orbital obliquity and axial-dipolar geomagnetic field from evaporite palaeolatitudes. *Nature* **444,** 51–55 (2006).
46. Donnadieu, Y., Fluteau, F., Ramstein, G., Ritz, C. & Besse, J. Is there a conflict between the Neoproterozoic glacial deposits and the snowball Earth interpretation: an improved understanding with numerical modeling. *Earth Planet. Sci. Lett.* **208,** 101–112 (2003).
47. Pollard, D. & Kasting, J. Climate-ice sheet simulations of Neoproterozoic glaciation before and after collapse to Snowball Earth. *Geophys. Monogr. Ser.* **146,** 91–105 (2004).
48. Lythe, M. *et al.* Bedmap: a new ice thickness and subglacial topographic model of Antarctica. *J. Geophys. Res.* **106,** 11335–11351 (2001).
49. Hoffman, P. F. Strange bedfellows: glacial diamictite and cap carbonate from the Marinoan (635) glaciation in Namibia. *Sedimentology* **58,** 57–119 (2011).

doi:10.1038/nature11894

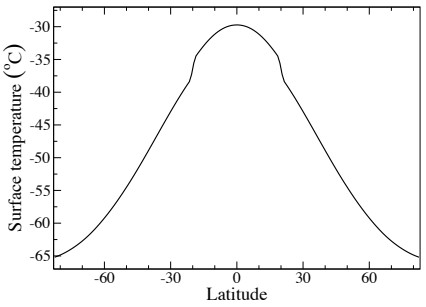

Figure SI-1: Atmospheric temperature as function of latitude, $T_s(y)$, specified at the top of the ice cover.

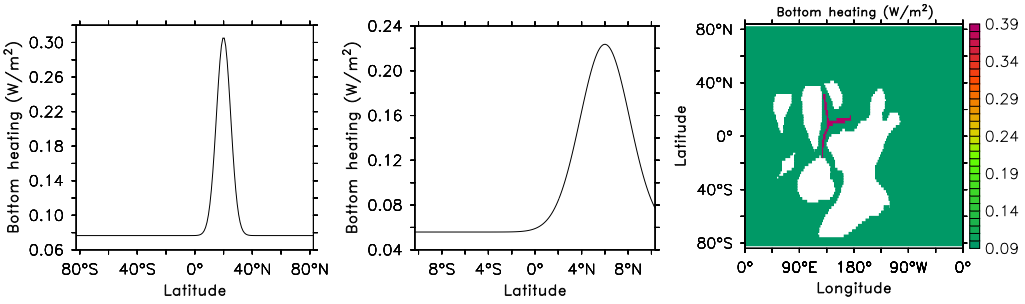

Figure SI-2: Geothermal flux forcing for the three experiments shown in the paper. (Left) 2D model. (Middle) high resolution model. (Right) global 3D model.

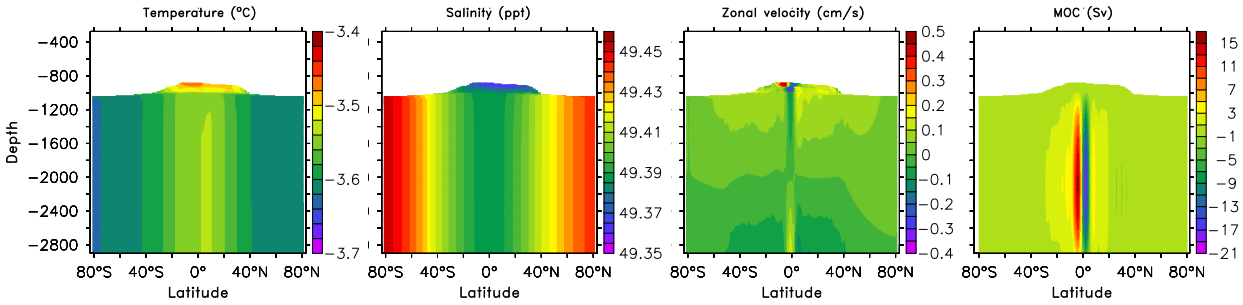

Figure SI-3: Zonally averaged temperature, salinity, zonal velocity and MOC for the 3D model shown in the paper. A comparison with Fig. 1 shows that the 2D and 3D models give similar zonal-averaged results, see discussion in the main text of the paper.